Paper 235

Proceedings of the Eleventh International Conference
on Computational Structures Technology,
B.H.V. Topping, (Editor),
Civil-Comp Press, Stirlingshire, Scotland

Optimal Fibre Reinforcement for Masonry Structures using Topology Optimization

M. Bruggi, G. Milani and A. Taliercio
Department of Structural Engineering
Politecnico di Milano, Milan, Italy

Abstract

A novel approach for the optimal positioning of fiber reinforcements in masonry structures is presented, based on topology optimization techniques [1]. Topology optimization has already been used to generate energy-based truss-like layouts that may be straightforwardly interpreted as strut-and-tie models in concrete structures [2]. The minimization of the so-called structural compliance allows optimal load paths to be defined, which may inspire a safe disposal of steel bars, provided that the structural element is sufficiently ductile.

Due to the brittle behaviour of masonry, the minimization of the strain energy cannot be adopted as an objective. The problem may be conveniently re-formulated as a minimization of the amount of reinforcement required to keep tensile stresses in any masonry element below a prescribed threshold. The strength criteria employed for masonry elements are formulated according to a recently presented lower bound limit analysis homogenization model [3], based on a discretization of a quarter of any unit cell by six CST elements. As a result of the limited number of variables involved, closed form solutions for the masonry macroscopic strength domain can be obtained. This calls for the adoption of a multi-constrained discrete formulation that locally controls the stress field over the whole design domain [4].

The contribution discusses preliminary numerical results addressing fibre-reinforcement of some benchmark masonry walls.

Keywords: masonry, fibre-reinforcement, topology optimization.

1 Introduction

In the last decades the use of fibre reinforced polymers (FRPs) for the retrofitting of existing buildings has become more and more widespread. Retrofitting can be motivated by the need of meeting current standards, or to protect a damaged structural element from further physical-chemical environmental aggression. The

first applications of this technique date probably back to the 90s and refer to concrete structures [5],[6]. FRP strips or sheets are mostly employed to externally reinforce cracked r.c. beams [7], or to wrap columns to enhance their mechanical performances under horizontal actions [8]. More recently, externally bonded FRP strips were also employed to retrofit or repair historic masonry buildings. This technique has several advantages over standard retrofitting techniques, including flexibility, effectiveness, and reversibility. Additionally, in the case of buildings in seismic regions, FRP strips do not significantly increase the structural mass and the earthquake-induced inertia forces, contrary to conventional techniques such as external reinforcements with steel plates, surface concrete coatings, and welded meshes.

Laboratory tests aimed at assessing the effectiveness of FRPs in enhancing the mechanical performances of masonry structures have been recently carried out e.g. by Foraboschi [9] on arches subjected to static loads, and by Grande et al. [10] and Capozucca [11] on walls subjected to cyclic loads. For an exhaustive and quite updated overview of the experimental researches carried out on masonry structural elements reinforced by FRPs, readers are referred to [12]. A critical issue when FRP strips are used to reinforce masonry elements is the effectiveness of the interfacial bonding. Delamination between externally bonded FRPs and masonry surfaces can nullify the strengthening effect of the reinforcement: this problem has been experimentally investigated e.g. by Aiello et al. [13] and Capozucca [14]. Appropriate surface treatments can avoid premature debonding at the masonry-FRP interface.

So far, the layout of the reinforcing FRP strips on laboratory samples or real structures has been basically driven by the intuition, owing to the simplicity of the loading conditions, or by the intent of healing existing cracks. A more rigorous approach relying upon structural mechanics and optimization might be necessary under complex load conditions or geometries. A preliminary attempt toward a mechanically sound design of the reinforcing path was made by Krevaikas et al. [15], who tried to identify on a rational basis the optimal layout of FRP strips on in-plane loaded masonry walls according to a strut-and-tie scheme.

In this paper, topology optimization is used as a tool to spot out the geometry of the layout of the reinforcing material that 'optimizes' any structural performance under given constraints, including an upper bound on the quantity of available reinforcement. In the applications shown hereafter, the objective function to be minimized is the volume (that is, the cost) of the reinforcements, but different choices are possible, e.g., the minimization of the highest tensile stress in the masonry element, or the maximization of the global stiffness or the load bearing capacity of the reinforced structure. In the optimization procedure, tensile strength of the masonry elements is limited according to a homogenized strength criterion recently presented in [3].

The outline of the paper is as follows. First, the limit analysis homogenization model used to derive the macroscopic strength properties of brickwork are briefly recalled in Section 2. This model will be employed to check the admissibility of the stress at any point of the masonry element to be reinforced. Then, the fundamentals of topology optimization are outlined; the mathematical problem to be solved to

achieve the optimal topology of reinforcement to be bonded to any masonry element under given external loads is formulated (Sec. 3). This technique spontaneously leads to identify an optimal pattern of reinforcement basically consisting of ties. One of the advantages of topology optimization is that no a-priori assumption regarding the position and the geometry of the reinforcing strips is required. The potentialities of the proposed approach are illustrated in Sec. 4 with reference to a technically meaningful case study. Finally, the main findings of the work are summarized and future perspectives of the research are outlined (Sec. 5).

2 Homogenization approach

The homogenized masonry behavior at failure is obtained by means of a simple equilibrated limit analysis model presented in [3], suitable to obtain masonry macroscopic in-plane failure surfaces with a rather limited computational effort. Due to the reduced number of optimization variables involved, any standard LP approach may be used, including simplex, active set and interior point methods, to obtain homogenized masonry yield domains.

The representative volume element Y (RVE, or elementary cell) depicted in Figure 1 is considered. Y contains all the information necessary to describe the macroscopic behavior of the entire wall completely. If a running bond pattern is considered, as shown in Figure 1, an elementary cell of rectangular shape can be conveniently adopted.

According to homogenization theory [16],[17],[18], averaged quantities representing the macroscopic stress and strain tensors ($\boldsymbol{E}$ and $\boldsymbol{\Sigma}$, respectively) are defined:

$$\boldsymbol{E} = <\boldsymbol{\varepsilon}> = \frac{1}{A}\int_Y \boldsymbol{\varepsilon}(\boldsymbol{u})dY \text{ and } \boldsymbol{\Sigma} = <\boldsymbol{\sigma}> = \frac{1}{A}\int_Y \boldsymbol{\sigma} dY \tag{1}$$

where A is the area of the 2D elementary cell, $\boldsymbol{\varepsilon}$ and $\boldsymbol{\sigma}$ stand for the local quantities (stresses and strains respectively) and <*> is the averaging operator.

The local stress ($\boldsymbol{\sigma}$) and displacement ($\boldsymbol{u}$) fields must fulfill suitable periodicity conditions that read:

$$\begin{cases} \boldsymbol{u} = \boldsymbol{E}\boldsymbol{y} + \boldsymbol{u}^{\text{per}} & \text{in} \quad Y \\ \boldsymbol{\sigma}\boldsymbol{n} \quad \text{anti-periodic} & \text{on} \quad \partial Y \end{cases} \tag{2}$$

where $\boldsymbol{u}^{\text{per}}$ is the periodic part of the displacement field, $\boldsymbol{y} = \{y_1, y_2, y_3\}$ is any point in the local reference frame, and ∂Y is the boundary of the RVE (see Figure 1).

In the model, joints are reduced to interfaces of vanishing thickness and blocks are discretized by means of a coarse mesh constituted by constant stress triangular elements (CST), as sketched in Figure 1. The choice of meshing a quarter of any brick through at least 3 triangular elements is due to the need of reproducing the

presence of shear stress in the bed joint (element 2 in Figure 1) under horizontal stretching. In principle, block failure can occur at the brick-to-brick interfaces. In this way and with the coarse discretization adopted, 1/4 of the RVE is meshed through 6 CST elements, indicated in Figure 1 as 1, 2, 3, 1', 2', 3'. The generalization of the symbols to the whole cell is straightforward.

From here onwards, the superscript $^{(n)}$ will indicate any stress component belonging to the n-th element. Accordingly, assuming the wall to undergo plane-stress conditions, the Cauchy stress tensor in the n-th CST element, $\boldsymbol{\sigma}^{(n)}$, is characterized by three non-vanishing components $\sigma_{xx}^{(n)}$ (horizontal stress), $\sigma_{yy}^{(n)}$ (vertical stress) and $\sigma_{xy}^{(n)}$ (shear stress).

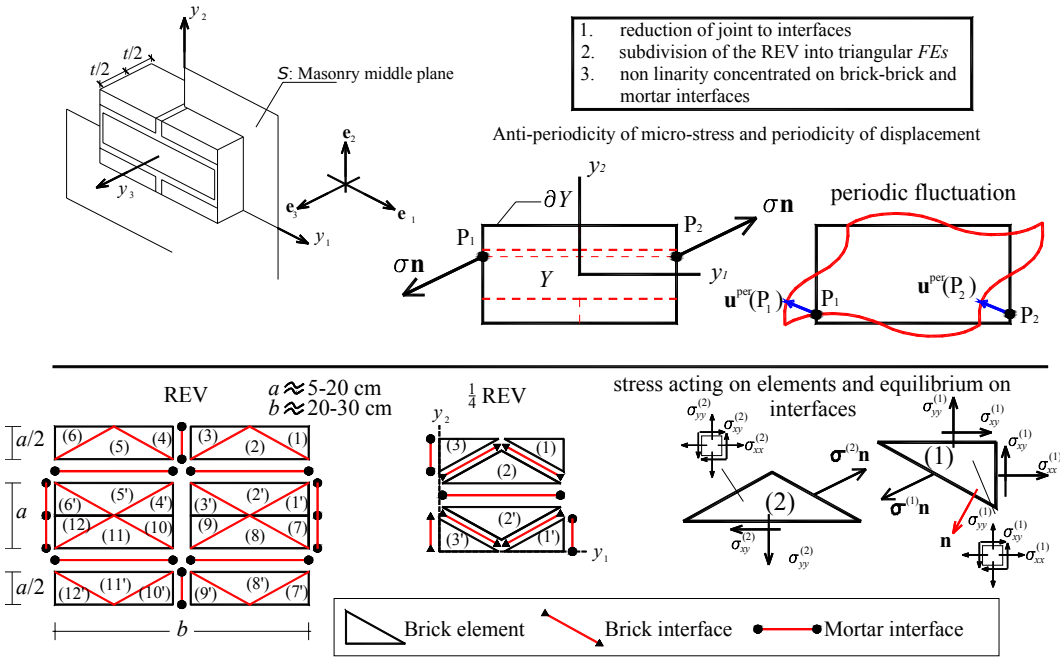

Figure 1. The micro-mechanical model proposed. Subdivision of the REV into 24 CST triangular elements (and 1/4 into 6 elements) and anti-periodicity of the micro-stress field

Referring to the static approach of limit analysis [19], equilibrium within any element is a-priori satisfied, being the stress tensor element-wise constant (div$\boldsymbol{\sigma}$ = **0**). On the contrary, two equality constraints involving stress components in adjoining triangular elements have to be prescribed at any internal interface. For instance, when dealing with the interface between elements1 and 2, the stress vector must be continuous from an element to the other. Thus, $\sigma_{xx}^{(2)} = \sigma_{xx}^{(1)} + \rho\left(\sigma_{xy}^{(1)} - \sigma_{xy}^{(2)}\right)$ and $\sigma_{yy}^{(2)} = \sigma_{yy}^{(1)} + \rho^{-1}\left(\sigma_{xy}^{(1)} - \sigma_{xy}^{(2)}\right)$, having denoted by ρ the ratio of the semi-length to the height of the brick ($\rho = b/2a$). Similar equations must be written for all the other interfaces, which are globally 28. A total of 56 equilibrium equations at the interfaces is obtained, whereas 73 are the unknowns of the problem: 72 stress components (three for each triangular element), and the load multiplier λ.

Anti-periodicity constrains for the stress vector are prescribed on the couples of triangles 1-6, 1'-6', 7-12, 7'-12', 1-7', 3-9', 4-10', 6-12', leading to additional 16 equalities. For instance, referring to couple 1-6, stress anti-periodicity amounts at setting $\sigma_{xx}^{(1)} = \sigma_{xx}^{(6)}$ and $\sigma_{xy}^{(1)} = \sigma_{xy}^{(6)}$.

Not all of the equations, however, are linearly independent. In particular, it can be shown that the corner elements 1, 6, 7 and 12 provide 4 linearly dependent equations for the shear stress.

To summarize, the optimization problem involves 73 unknowns, 68 linearly independent equations, and a set of inequality constraints representing the yield conditions at the interfaces and involving unknown stress components. The objective function, in the framework of the lower bound theorem of limit analysis, is simply the load multiplier.

To estimate a single point of the homogenized yield domain, it is thus necessary to solve the following linear programming (LP) problem:

$$\max \lambda \qquad \text{subject to} \begin{cases} \lambda\alpha = \dfrac{\sum_{i=1}^{24} \sigma_{xx}^{(i)} A_i}{2ab} \\ \lambda\beta = \dfrac{\sum_{i=1}^{24} \sigma_{yy}^{(i)} A_i}{2ab} \\ \lambda\gamma = \dfrac{\sum_{i=1}^{24} \sigma_{xy}^{(i)} A_i}{2ab} \\ \boldsymbol{A}_{eq}^{I} \boldsymbol{X} = \boldsymbol{b}_{eq}^{I} \\ \boldsymbol{A}_{eq}^{ap} \boldsymbol{X} = \boldsymbol{b}_{eq}^{ap} \\ f_E^i\left(\sigma_{xx}^{(i)}, \sigma_{yy}^{(i)}, \tau^{(i)}\right) \le 0, \ i = 1...24 \\ f_I^i\left(\sigma_I^{(i)}, \tau_I^{(i)}\right) \le 0, \ i = 1...32 \end{cases} \tag{3}$$

The symbols used in equation (3) have the following meaning:

- α, β and γ indicate the components of the unit vector $\boldsymbol{n}_\Sigma$, see Figure 2, in the homogenized membrane stress space;
- A_i is the area of the i-th element (ab/8 or ab/16);
- $\boldsymbol{X}$ is a 73×1 array, gathering all the LP problem unknowns (element stress components and collapse multiplier);
- $\boldsymbol{A}_{eq}^{I}\boldsymbol{X} = \boldsymbol{b}_{eq}^{I}$ is a set of linear equations collecting equilibrium constraints on all the interfaces. $\boldsymbol{A}_{eq}^{I}$ is a 56×73 matrix and $\boldsymbol{b}_{eq}^{I}$ is a 56×1 array with entries equal to zero;
- $\boldsymbol{A}_{eq}^{ap}\boldsymbol{X} = \boldsymbol{b}_{eq}^{ap}$ collects the anti-periodicity conditions and it is therefore a set of 16 equations (some of them linearly dependent). Thus $\boldsymbol{A}_{eq}^{ap}$ is a 16×73 matrix and $\boldsymbol{b}_{eq}^{ap}$ is a 16×1 array with entries equal to zero;

- $\boldsymbol{f}_E^i\left(\sigma_{xx}^{(i)},\sigma_{yy}^{(i)},\sigma_{xy}^{(i)}\right)\leq \mathbf{0}$ is a set of possibly non-linear inequalities constraints representing the failure surface adopted for the *i*-th element;
- $\boldsymbol{f}_I^i\left(\sigma_I^{(i)},\tau_I^{(i)}\right)\leq \mathbf{0}\ \ \forall i=1,...,32$ plays the role of $\boldsymbol{f}_E^i$ for the interfaces, with $\sigma_I^{(i)}$ and $\tau_I^{(i)}$ indicating respectively the normal and shear stress acting on the *i*-th interface.

The solution of the optimization problem (3) allows a point on the homogenized failure surface to be determined, having coordinates $\Sigma_{xx} = \alpha\lambda$, $\Sigma_{yy} = \beta\lambda$ and $\Sigma_{xy} = \gamma\lambda$. Traditionally, sections of the masonry failure surface are obtained assuming a fixed angle θ between the bed joints and the macroscopic principal horizontal stress (Σ_{11}) and varying the angle $\psi = \tan^{-1}\Sigma_{22}/\Sigma_{11}$, where Σ_{22} is the macroscopic vertical stress. The components of vector $\boldsymbol{n}_\Sigma$ can be expressed as:

$$
\begin{aligned}
n_\Sigma(1) &= \frac{1}{2}\left(\cos(\psi)(1+\cos(2\theta))+\sin(\psi)(1-\cos(2\theta))\right)\\
n_\Sigma(2) &= \frac{1}{2}\left(\cos(\psi)(1-\cos(2\theta))+\sin(\psi)(1+\cos(2\theta))\right)\\
n_\Sigma(3) &= \frac{1}{2}\left(\cos(\psi)\cos(2\theta)-\sin(\psi)\cos(2\theta)\right)\tan(2\theta)
\end{aligned}
\tag{4}
$$

Two typologies of interfaces are present in the model, namely brick-to-brick interfaces and mortar joints. Whereas non-linear failure surfaces may be easily dealt with within a LP scheme (abundant literature is available [20]), here bricks are assumed to be infinitely strong and joints are reduced to interfaces with a Mohr-Coulomb failure criterion, with tension cutoff and linear cap in compression. Hence, constituent material failure surfaces are already linear, and no linearization routines are needed.

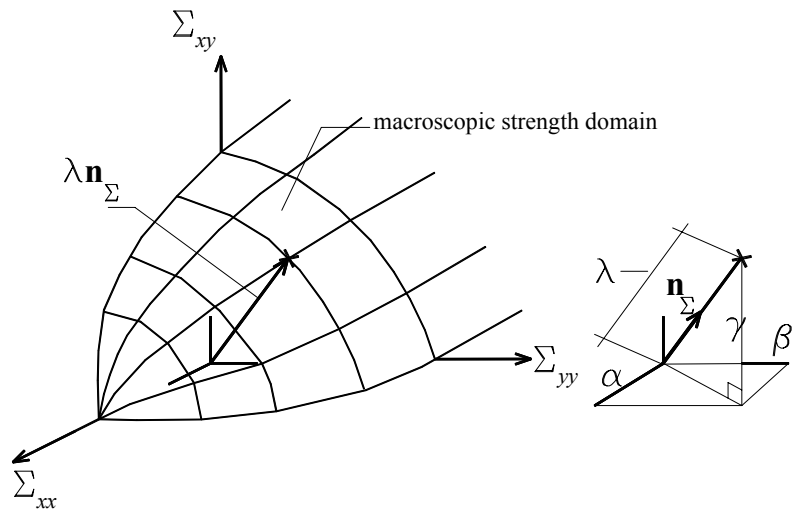

Figure 2. General in-plane load: meaning of multiplier λ in the homogenized stress space ($\Sigma_{xx} = n_\Sigma(1)$, $\Sigma_{yy} = n_\Sigma(2)$ and $\Sigma_{xy} = n_\Sigma(3)$)

A discussion on the effects of the linearization of possibly non-linear failure surfaces is beyond the scope of the present paper and is, in any case, a classic issue that has been extensively treated in specialized literature.

(3) is a standard LP problem, which allows the collapse load of any structure to be estimated within the FE approach, as stated for the first time in Anderheggen and Knopfel [20].

Readers are referred e.g. to [21]-[24] for a critical discussion of efficient (classical) LP and to[22]-[24] for conic programming tools suited for solving (3).

3 The topology optimization problem

In view of a finite element discretization of the optimization problem, let consider a discrete plane stress model for any masonry element subjected to prescribed loads and constraints. Under the assumption of perfect bonding, a fibre-reinforced layer may be modeled as an additional in-plane stiffness contribution to the underlying brickwork. Extending the framework of conventional approaches for topology optimization (see e.g. [25],[26]), one may define two arrays of element-wise minimization unknowns, i.e. x_i and θ_i, which govern the stiffness of the reinforced structure according to the following expression:

$$\boldsymbol{K}_{Ti}(x_i, \theta_i) = \boldsymbol{K}_{Mi} + x_i^p \boldsymbol{K}_{Ri}(\theta_i). \tag{5}$$

In the above expression, $\boldsymbol{K}_{Ti}$ is the element plane stress matrix modeling both masonry and reinforcement. $\boldsymbol{K}_{Ti}$ includes the contribution of the underlying masonry structure, $\boldsymbol{K}_{Mi}$, along with the term accounting for the fibre-reinforcement, $\boldsymbol{K}_{Ri}$. $\boldsymbol{K}_{Ri}$ depends on the orientation of the fibres, θ_i, and is scaled to the (normalized) density of the reinforcement x_i through the so-called SIMP law that implements a penalization with exponent p, see 0. The proposed approach allows any optimization problem to be dealt with resorting to continuous functions for the density unknowns $0 \leq x_i \leq 1$, while stiffness penalization at intermediate density is able to steer the solution towards the expected extreme values of the range. The terms $\boldsymbol{K}_{Mi}$ and $\boldsymbol{K}_{Ri}$ are both computed taking into account the orthotropic features of the materials. To model a fibre-reinforcement exhibiting a prevailing stiffness along a single direction, a vanishing elastic modulus is considered in the direction perpendicular to the fibres. The possible orientations of the fibres, θ_i, are unconstrained.

The optimal layout of fibre-reinforcement is defined by the distribution of reinforcing material, along with the relevant orientation of its fibres, that minimize the weight of the added phase and make the stress regime throughout the whole underlying masonry structure admissible according to the criterion defined in the previous Section. The discrete version of the topology optimization problem implemented in this work may be therefore written as:

$$
\begin{cases}
\min\limits_{\boldsymbol{x},\boldsymbol{\theta}} \sum\limits_{i=1}^{n} x_i A_i \ \text{ s.t.} \\
\left(\boldsymbol{K}_M + x^p \boldsymbol{K}_R(\boldsymbol{\theta})\right)\boldsymbol{u} = \boldsymbol{f} \\
\boldsymbol{F}_M(\boldsymbol{\sigma}_{Mj}) \le 0, \quad j = 1,\ldots,m \\
0 \le x_i \le 1, i = 1,\ldots,n \\
0 \le \theta_i \le \pi, \quad i = 1,\ldots,n
\end{cases}
\tag{6}
$$

The objective function of the above equation is the weight of the reinforcement, being A_i the area of the i-th finite element, x_i the corresponding density unknown, and n the number of finite elements. Recall that any element is also related to the additional optimization unknown θ_i, defining the local orientation of the fibres. Reference is also made to free material optimization for additional details on the optimal design involving anisotropic materials, see e.g. [27]. The first constraint of the optimization problem enforces the equilibrium equation for the reinforced structural element in weak form, within the framework of a classical displacement-based formulation. The global stiffness matrix may be split into two contributions related to the underlying masonry element $\boldsymbol{K}_M$ and the overlying fibre-reinforcement $\boldsymbol{K}_R$, in full agreement with the above discussion on element-wise contributions. The second requirement consists of a sets of local constraints that enforce the strength criterion presented in the previous Section, involving the components of the stress tensor in the masonry layer. This is defined as $\boldsymbol{\sigma}_{Mj}$ when referring to the j-th element. The term $\boldsymbol{\sigma}_{Mj}$ may be computed at the centroid of each finite element moving from the displacement field derived at equilibrium by means of a post-processing computation that recovers the strain regime in the masonry layer. All the inequalities prescribed by the adopted strength criteria are evaluated for each finite element to be constrained, while only a few are implemented as effective enforcements according to the selection strategy presented in [25]. This approach allows the number of active constraints to be significantly reduced, as a very limited set of local enforcements ($m \ll n$) may be selected and included in the optimization to provide an affordable and efficient solution of the multi-constrained minimization problem. Since stress-constraints are enforced on a fixed phase of the domain, i.e. the masonry layer, the well-known singularity problem does not affect the minimization procedure and no relaxation is required to handle stress constraints, see e.g. [28].

The presented optimization problem is solved by means of mathematical programming, see [29], and calls for the sensitivity analysis of objective function and constraints on the two sets of variables, i.e. x_i and θ_i. The starting guess for the density unknowns consists of a full reinforcement of the structural element, which means $x_i = 1$ all over the domain. The initial orientation of the fibres matches the direction related to the tensile principal stresses of the unreinforced masonry. Indeed, the optimal fibre direction is strictly related, but not equal, to the direction of the tensile principal stresses of the underlying element. This will be further discussed in the next section.

4 Numerical simulations

Let consider a square masonry panel with edge $L = H$ equal to 3 m and thickness s = 0.12 m. The panel is supposed built with standard Italian bricks of dimensions 250×55 mm (length × height) and joints 10 mm thick, reduced to interfaces in the model for the sake of simplicity. The wall is supposed to be connected to the ground by means of two rigid regions at the corners of the lower side, enforcing vanishing displacements along both the horizontal and the vertical direction. A vertical force P = 10 kN is distributed along the central region of the upper side of the specimen that is discretized by means of about 4000 square elements. The Young modulus of the brickwork in the horizontal direction is denoted E_1=1412 MPa, while in the vertical direction one has E_2=1050 MPa. Additionally, the Poisson ratio ν_{12} is taken equal to 0.1762 and the shear modulus G_{12}=367 MPa.

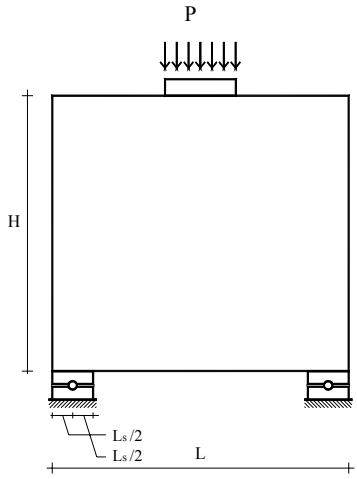

Figure 3. Geometry of the deep beam analyzed

The presented formulation for the topology optimization of fibre-reinforcement is implemented with the aim of distributing and orienting the minimum amount of material for an overlying layer of thickness t_F = 0.2 mm and Young modulus E = 160 GPa along the fibre direction. The stress regime in the reinforced masonry panel must fully comply with the strength criterion presented in Sec. 2.

Homogenized failure surface sections at different orientations of the bed joint to the principal stress Σ_{11}, utilized for masonry at a structural level and derived from the equilibrated and admissible model previously described, are schematically depicted in Figure 4. Only the tension-tension region is represented, as the optimization performed at a structural level requires a limitation of the positive stresses at the interface.

The following parameters have been used for joints reduced to interfaces: cohesion c = 0.103 MPa, tension cutoff f_t = 0.103 MPa, and friction angle Φ = 30°. The implemented selection strategy spots out a limited set of governing constraints, which drive the procedure by progressively removing element-wise fibre-reinforcement contributions. No more than 50 constraints are active throughout the optimization procedure.

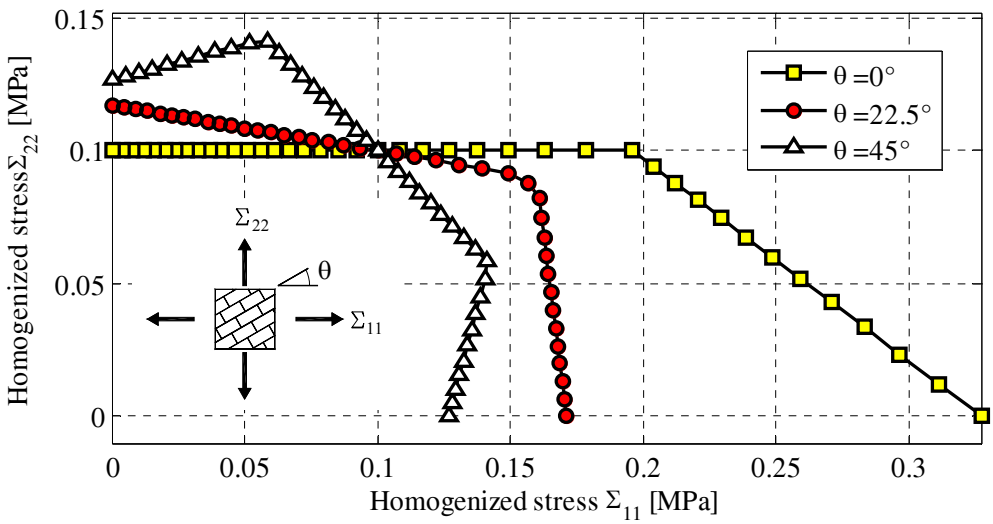

Figure 4. Masonry homogenized failure surface sections at different orientations of the bed joints with respect to material axes

The minimum weight solution that is admissible with respect to the selected masonry strength criterion is presented in Figure 5 and Figure 6. Figure 5 shows the optimal distribution of fibre-reinforcing material (black regions stand for fibre-reinforced zones), while the optimal orientation of the fibres is depicted in Figure 6. Looking for regions which share a nearly homogeneous distribution in terms of fibre orientation, one may easily identify the optimal layout of FRP "stripes" to be plated on the masonry panel. This is in full agreement with the adoption of energy-based optimization procedures to define equilibrated truss-like model, which can be interpreted as strut-and-tie models in concrete elements, see e.g. [29]. A horizontal stripe should be prescribed at the bottom of the specimen to reduce horizontal tensile stresses. Additionally, V-shaped stripes should be conveniently introduced to hang up the fraction of vertical load supported by this highly-stressed region. Figure 7 shows contour plots of the difference between the optimal orientation of fibres and the direction of the tensile principal stresses in the unreinforced element (angles measured in sexagesimal degrees). As one may easily see, the optimal orientation of the fibres is related to the direction of the tensile principal stresses of the underlying panel, which may be therefore conveniently implemented as starting guess for the array $\boldsymbol{\theta}$ in the optimization procedure.

5 Conclusions

A novel procedure was proposed to achieve the optimal layout of FRP reinforcements for masonry structures based on a rigorous topology optimization approach. Unlike existing procedures [15], which assume *a-priori* a sort of mesh through which the optimal reinforcing array has to pass , in the proposed approach the layout of the reinforcement is completely free.

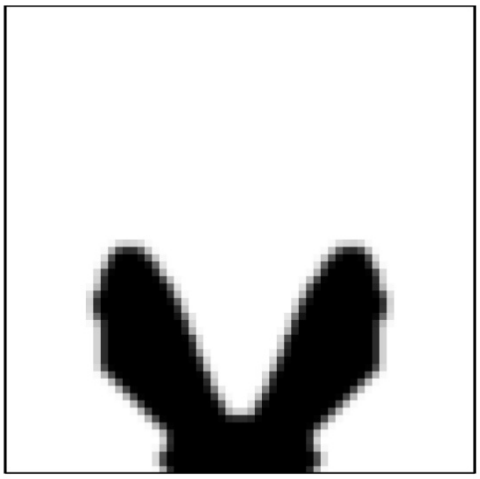

Figure 5. Optimal distribution of fibre-reinforcement

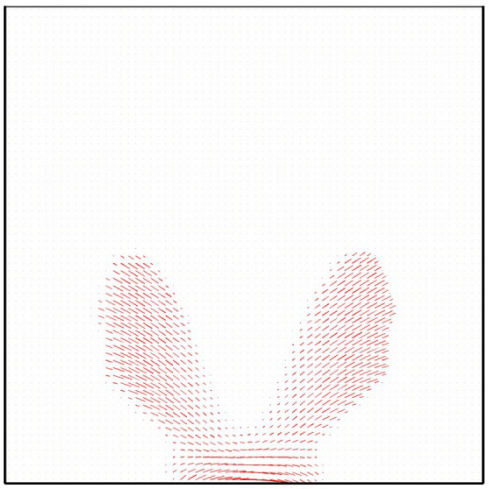

Figure 6. Optimal fibre orientation of the reinforcement plotted in Figure 5

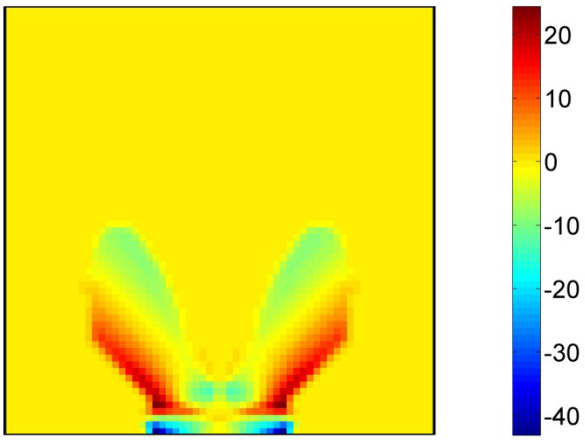

Figure 7. Difference between the optimal orientation of the fibres and the direction of the maximum (tensile) principal stress in the underlying brickwork (angles measured in sexagesimal degrees)

This procedure can be virtually applied to any masonry element, irrespective of the complexity of its geometry. Existing cracks can also be taken into account. The choice of the objective function and the constraints can be modified, to comply with any requirements of the designer. For instance, the global structural stiffness, or its bearing capacity, could be maximized for a prescribed quantity of reinforcement, keeping the stress in the masonry element below a certain threshold, and so on.

In the current version, the reinforcing array is assumed to consist of unidirectional FRPs: future extension of the research entail the extension of the proposed procedure to multidirectional reinforcements, which are often employed in the applications. Also, the sensitivity of the optimal layout to the choice of the strength criterion employed for the unreinforced masonry should be estimated. Another important issue that has to be dealt with in the prosecution of the research is the control of the inter-laminar shear stresses, which are responsible for the

debonding of the reinforcing layers: these stresses require structural theories more accurate than the plane stress analysis employed so far to be captured. Finally, the possibility of assessing the effectiveness of the numerically obtained layouts through experiments on full scale reinforced masonry specimens has been planned.

References

[1] M. Bendsøe, N. Kikuchi, "Generating optimal topologies in structural design using a homogenization method", Comp. Meth. Appl. Mech. Eng., 71, 197-224, 1988.

[2] M. Bruggi, "Generating strut-and-tie patterns for reinforced concrete structures using topology optimization", Comp. Struct., 87, 1483-1495, 2009.

[3] G. Milani, "Simple homogenization model for the non-linear analysis of in-plane loaded masonry walls", Comput. Struct., 89, 1586-1601, 2011.

[4] P. Duysinx, M.P. Bendsøe, "Topology optimization of continuum structures with local stress constraints", Int. J. Numer. Methods Eng., 43, 1453-1478, 1998.

[5] T. Norris, H. Saadatmanesh, M.R. Eshani, "Shear and flexural strengthening of r/c beams with carbon fibers sheets", ASCE-J. Struct. Eng., 123(7), :903-911, 1997.

[6] T.C. Triantafillou, "Shear strengthening of reinforced concrete beams using epoxy-bonded FRP composites", ACI-Struct. J., 95(2), 107-115, 1998.

[7] M. Arduini, A. Nanni, "Behavior of precracked r.c. beams strengthened with carbon FRP sheets", J. Compos. Constr., 1(2), 63-70, 1997.

[8] M. Shahawya, A. Mirmiranb, T. Beitelman, "Tests and modeling of carbon-wrapped concrete columns", Composites: Part B, 31(6-7), 471-480, 2000.

[9] P. Foraboschi, "Strength assessment of masonry arch retrofitted using composite reinforcements", Masonry Int., 15(1), 17-25, 2001.

[10] E. Grande, G. Milani, E. Sacco, "Modelling and analysis of FRP-strengthened masonry panels", Engng. Struct., 30(7), 1842-1860, 2008.

[11] R. Capozucca, "Experimental analysis of historic masonry walls reinforced by CFRP under in-plane cyclic loading", Compos. Struct., 94, 277-289, 2011.

[12] N.G. Shrive, "The use of fibre reinforced polymers to improve seismic resistance of masonry", Constr. Build. Mat., 20(4), 269-277, 2006.

[13] M.A. Aiello, M.S. Sciolti, "Analysis of bond performance between FRP sheets and calcarenite stones under service and ultimate conditions" Masonry Int., 21(1), 15-28, 2008.

[14] R. Capozucca, "Experimental FRP/SRP-historic masonry delamination", Compos. Struct., 92, 891-903, 2010.

[15] T.D. Krevaikas, T.C. Triantafillou, "Computer-aided strengthening of masonry walls using fibre-reinforced polymer strips", Mater. Struct., 38, 93-98, 2005.

[16] P. Pegon, A. Anthoine, "Numerical strategies for solving continuum damage problems with softening: application to the homogenisation of masonry", Comput. Struct., 64(1-4), 623-642, 1997.

[17] A. Anthoine, "Derivation of the in-plane elastic characteristics of masonry through homogenization theory", Int. J. Solids Struct. 32(2), 137-163, 1995.

[18] R. Luciano, E. Sacco, “Damage of masonry panels reinforced by FRP sheets”, Int. J. Solids Struct., 35(15), 1723-1741, 1998.
[19] P. Suquet, “Analyse limite et homogénéisation”, Comptes Rendus de l’Académie des Sciences – Série IIB – Mécanique, 296, 1355-1358, 1983.
[20] E. Anderheggen, H. Knopfel, “Finite element limit analysis using linear programming”, Int. J. Solids Struct., 8, 1413-1431, 1972.
[21] S.W. Sloan, “A steepest edge active set algorithm for solving sparse linear programming problems”, Int. J. Numer. Methods Eng., 12, 61-67, 1988.
[22] K. Krabbenhoft, A.V. Lyamin, M. Hjiaj, S.W. Sloan, “A new discontinuous upper bound limit analysis formulation”, Int. J. Numer. Methods Eng., 63, 1069-1088, 2005.
[23] A. Makrodimopoulos, C.M. Martin, “Lower bound limit analysis of cohesive frictional materials using second-order cone programming”, Int. J. Numer. Methods Eng., 66(4), 604-634, 2006.
[24] K. Krabbenhoft, A.V. Lyamin, S.W. Sloan, “Formulation and solution of some plasticity problems as conic programs”, Int. J. Solids Struct., 44, 1533-1549, 2007.
[25] M. Bruggi, P. Duysinx, “Topology optimization for minimum weight with compliance and stress constraints”, Struct. Multidiscip. Optim., doi:10.1007/s00158-012-0759-7, 2012 (in press).
[26] M.P. Bendsøe, O. Sigmund, “Topology Optimization - Theory, Methods and Applications”, Springer, Berlin, 2003.
[27] M.P. Bendsøe, J.M. Guades, R.B. Haber, P. Pedersen, J.E. Taylor, “An analytical model to predict optimal material properties in the context of optimal structural design”, J. Appl. Mech., 61, 930-937, 1994.
[28] M. Bruggi, “On an alternative approach to stress constraints relaxation in topology optimization”, Struct. Multidiscip. Optim., 36, 125-141, 2008.
[29] K. Svanberg, “Method of moving asymptotes - A new method for structural optimization”, Int. J. Numer. Methods Eng., 24, 359-373, 1987.